

# Three-Helix Bundle DNA Tiles Self-Assemble into 2D Lattice or 1D Templates for Silver Nanowires

Sung Ha Park,<sup>†,‡</sup> Robert Barish,<sup>†</sup> Hanying Li,<sup>†,§</sup> John H. Reif,<sup>†</sup> Gleb Finkelstein,<sup>‡</sup> Hao Yan,<sup>\*,||</sup> and Thomas H. LaBean<sup>\*,†</sup>

*Department of Computer Science, Department of Physics, and Department of Pathology, Duke University, Durham, North Carolina 27708, and Department of Chemistry and Biochemistry, Arizona State University, Tempe, Arizona 85287*

Received January 18, 2005; Revised Manuscript Received February 17, 2005

## ABSTRACT

We present a DNA nanostructure, the three-helix bundle (3HB), which consists of three double helical DNA domains connected by six immobile crossover junctions such that the helix axes are not coplanar. The 3HB motif presents a triangular cross-section with one helix lying in the groove formed by the other two. By differential programming of sticky-ends, 3HB tiles can be arrayed in two distinct lattice conformations: one-dimensional filaments and two-dimensional lattices. Filaments and lattices have been visualized by high-resolution, tapping mode atomic force microscopy (AFM) under buffer. Their dimensions are shown to be in excellent agreement with designed structures. We also demonstrate an electroless chemical deposition for fabricating metallic nanowires templated on self-assembled filaments. The metallized nanowires have diameters down to 20 nm and display Ohmic current–voltage characteristic.

Widely known for storage of genetic information in biology, DNA has also been recognized as a useful building material in the field of nanotechnology.<sup>1,2</sup> DNA provides basic building blocks for constructing functionalized nanostructures with four major features: molecular recognition, self-assembly, programmability, and predictable nanoscale structure. The limitations of conventional methods of top-down fabrication make bottom-up self-assembled nanostructures using DNA molecules an attractive technique for near-term nano/biotechnologies. Recently, self-assembled DNA nanostructures have been reported with several unique applications such as generating periodic lattices<sup>3–7</sup> for templates and scaffolds, constructing nanomechanical devices,<sup>8–10</sup> and computing systems.<sup>11,12</sup> Previous DNA tiles with parallel helices (DX and TX) have had coplanar helix axes which facilitate 2D tile arrays but show less promise for 3D lattices. The DNA tile reported here contains dsDNA domains out of the 2D lattice plane, which should be useful for tiling into the third dimension.

In this letter, we present a newly conceived motif, the three helix bundle (3HB), which consists of three double helical DNA domains joined in cyclic fashion at six strand-exchange

points, with two crossover junctions between each pair of helices. Using DNA's inherent programmability, molecular recognition, and self-assembly characteristics, we have designed and constructed simple but unique DNA nanostructures: 1D-3HB tiles for formation of one-dimensional chains or filaments of tiles and 2D-3HB for assembly of two-dimensional tile lattices. A 1D-3HB tile consists of nine different oligos which, when hybridized by slow annealing, form a bundle with three duplex domains connected by six immobile crossover junctions. Neighboring crossover points involve opposite strands of DNA, therefore dihedral angles between crossovers are calculated to be  $60^\circ$  since the minor groove gives us  $-146^\circ$ , and then six base-spacings of  $34.3^\circ$  each gives  $+206^\circ$ , for a rotation around the helix axis of  $-146^\circ + 6(34.3^\circ) = 60^\circ$ . A schematic diagram of the strand trace and a cartoon of the self-assembled 1D filament are shown in Figure 1a and 1b. The unit length of a 1D-3HB tile is  $\sim 17.0$  nm, which corresponds to five full turns of the helices (52 base pairs). The complementary sticky-ends of  $a$ ,  $b$ , and  $c$  are  $a'$ ,  $b'$ , and  $c'$ , thus 1D-3HB tiles hybridize into a single layer linear array, forming 1D filaments as shown.

2D-3HB tiles also consist of nine strands but have only 4.5 full turns of double helix (47 base pairs), for a unit length of  $\sim 15.3$  nm. A schematic diagram of a tile and a cartoon of self-assembled 2D lattice are shown in Figure 1c and 1d. Figure 1e is a front view of an atomic-scale model of the

\* Corresponding authors. (H.Y.): Phone: (480) 727-8570; Fax: (480) 965-2747; E-mail: hao.yan@asu.edu. (T.H.L.): Phone: (919) 660-6553; Fax: (919) 660-6519; E-mail: thl@cs.duke.edu.

<sup>†</sup> Department of Computer Science, Duke University.

<sup>‡</sup> Department of Physics, Duke University.

<sup>§</sup> Department of Pathology, Duke University.

<sup>||</sup> Department of Chemistry and Biochemistry, Arizona State University.

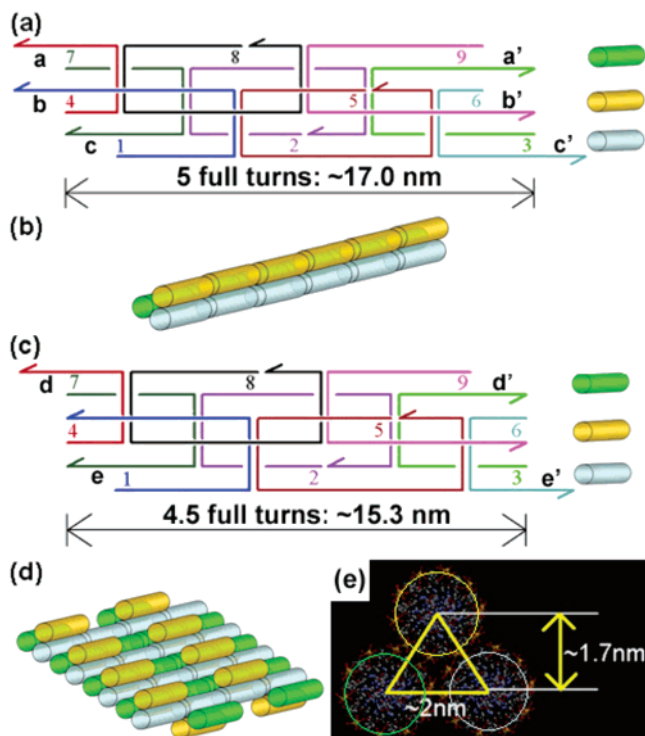


**Figure 1.** Schematic drawings of self-assembled 1D and 2D-3HBs. (a) 1D-3HB has nine different oligonucleotides which form 3-helix bundles with six crossovers. Different color-coded arrows indicate simplified strands running from 5' to 3'. Unit length of 1D-3HB is  $\sim 17$  nm. Here, the complementary sticky-ends of *a*, *b*, and *c* are *a'*, *b'*, and *c'* respectively. Identification of the three helices in the strand trace diagram with the helices of the simple tube cartoons are given by the color coded tubes to the right. (b) A cartoon of filaments formed from 1D-3HB tiles. (c) 2D-3HB also consists of nine different strands but is 4.5 full turns,  $\sim 15.3$  nm. The odd number of helical half-turns causes neighboring tiles to face alternating directions in the lattice plane. The complementary sticky-ends of *d* and *e* are *d'* and *e'*, respectively. (d) A cartoon of 2D-3HB lattice. (e) Front view of an atomic scale model of a 3HB tile. Because the diameter of double-stranded DNA is  $\sim 2$  nm, the height distance between centers of the lower duplexes and the upper is  $\sim 1.7$  nm.

3HB tile looking down the helix axes. The odd number of helical half-turns in 2D-3HB tiles provides alternate facings of adjacent tiles (as shown in Figure 1d) in the east-west direction in the lattice plane, giving the 2D array a so-called corrugated design. We intentionally removed the sticky ends of the out-of-plane helix domains (yellow cylinders in Figure 1c) and matched the complementary sequences of the other two as shown in Figure 1c. This slight reprogramming of the DNA molecules changes the resulting superstructure morphology dramatically from uniform 1D filaments to 2D lattices with upward- and downward-facing stripes. Base sequences of the oligonucleotides can be found in the Supporting Information (Figure S1).

Formation of single species with expected molecular weights and designed strand stoichiometry was demonstrated using gel electrophoresis of 3HB tiles without appended sticky ends (Figure 2). Thermal stability was also demonstrated; melting curves show a cooperative unfolding with a  $T_m$  of  $\sim 57$  °C (data shown in the Supporting Information, Figure S3). The DNA nanostructures have been visualized

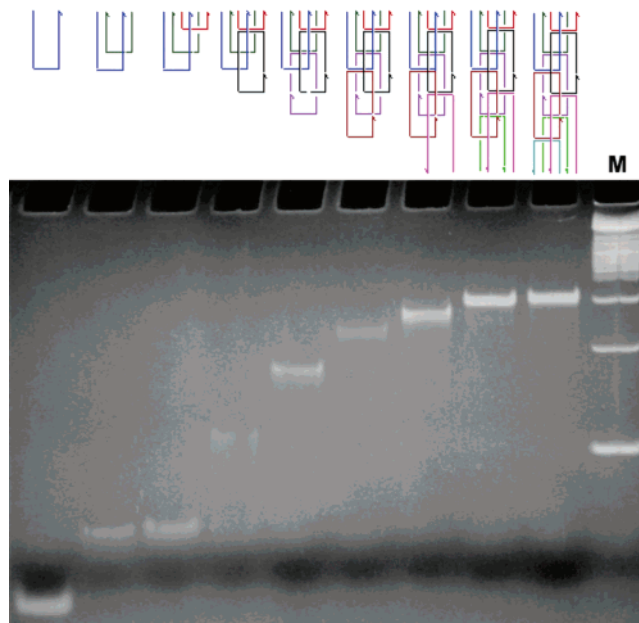


**Figure 2.** Characterization of the 3HB tile structure using non-denaturing electrophoresis. A 10% polyacrylamide gel (ethidium bromide stained) showing association complexes between various equimolar combinations of the 3HB DNA complex component strands. Equimolar mixtures at  $1 \mu\text{M}$  concentration per included strand were annealed and run on the gel at room temperature. Strands included in the annealings are indicated in the drawing above each lane. The last lane contains 50 bp DNA ladder size markers (M).

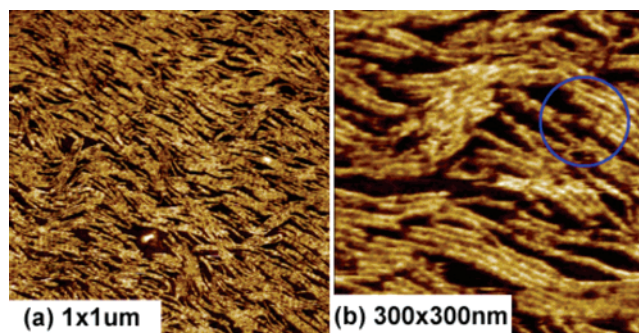


**Figure 3.** (a) AFM images of 1D-3HB filaments. Height of individual filaments is  $2.0 \pm 0.2$  nm, and length varies from a few hundreds nanometers to a few microns. (b) High-resolution AFM image of the filaments with  $300 \text{ nm} \times 300 \text{ nm}$  scan size. Individual unit tiles with a length of  $\sim 16.5$  nm can be seen clearly (circled in blue).

by atomic force microscopy, which provides high-resolution imaging (down to  $\sim 2$  nm). Figure 3a and 3b show AFM images of 1D filaments with scan sizes  $1 \mu\text{m} \times 1 \mu\text{m}$  and  $300 \text{ nm} \times 300 \text{ nm}$ , respectively. AFM images were taken using tapping mode under physiological buffer as described in the Supporting Information. The images show many individual filaments crowded together on the mica surface. Filaments have measured heights of  $1.8 \pm 0.2$  nm, and their lengths vary from a few hundred nanometers to a few microns (tens to hundreds of tiles). In high-resolution AFM images of filaments (Figure 3b), we clearly see individual 1D-3HB tiles (circled in blue) with a length of  $\sim 16.5$  nm, in good agreement with the original design of  $\sim 17.0$  nm.

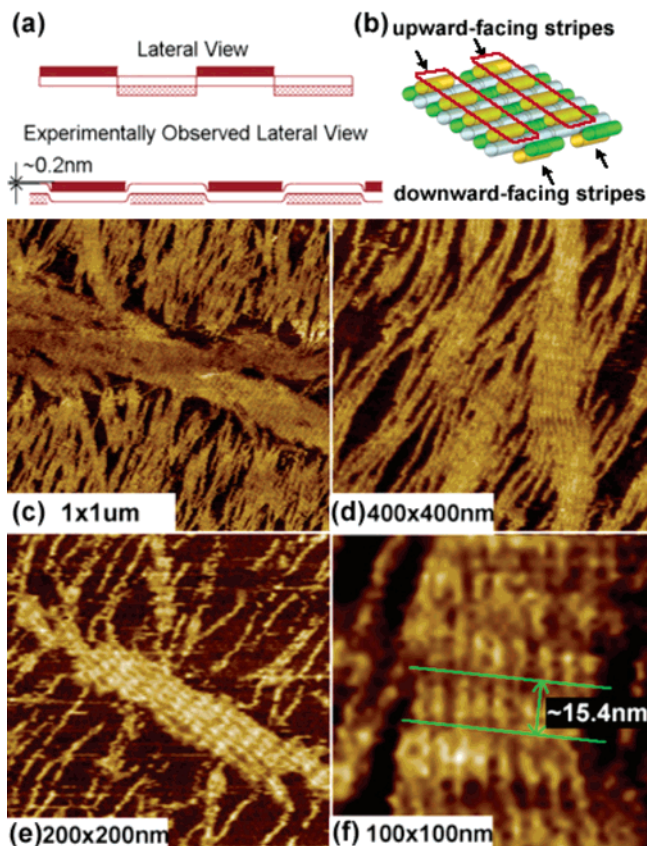


**Figure 4.** (a) Schematic diagrams of a 2D-3HB lattice rigid model lateral view (top) and a lateral view of a more flexible model closer to the experimental observations (bottom). (b) Cartoon of lattices with upward- and downward-facing stripes highlighted. (c–f) AFM images of the 2D-3HB lattices. Scan size of images are (c)  $1 \mu\text{m} \times 1 \mu\text{m}$ , (d)  $400 \text{ nm} \times 400 \text{ nm}$ , (e)  $200 \text{ nm} \times 200 \text{ nm}$ , and (f)  $100 \text{ nm} \times 100 \text{ nm}$ . 2D-3HB tiles are clearly visible and average length of the tiles is  $\sim 15.4 \text{ nm}$ .

Height measurements of the filaments can be found in the Supporting Information (Figure S4).

A schematic diagram of 2D-3HB lattice shown as a rigid model in lateral view is given in Figure 4a (top). Experimentally we observed a more flexible lattice with upward-facing stripes sagging slightly lower to the substrate as shown in Figure 4a (bottom). The height of upward-facing stripes is  $\sim 2.5 \text{ nm}$  and that of downward-facing stripes is  $2.3 \text{ nm}$ , measured from the mica surface. Thus the experimentally determined height difference between alternating stripes is  $\sim 0.2 \text{ nm}$ . Height analysis AFM images are given in the Supporting Information (Figure S5). The cartoon in Figure 4b highlights the different stripes observed on the lattices. Figures 4c through 4f show high-resolution AFM images of 2D lattices. From AFM images, 2D-3HB tiles and stripes are clearly visible; the average length of the tiles is  $\sim 15.4 \text{ nm}$ , in excellent agreement with the designed distance of  $\sim 15.3 \text{ nm}$ .

Direct electrical transport measurements in DNA molecules have been considered an interesting research subject for the past few decades. Even though some conductivity experiments with DNA have shown semiconducting<sup>13</sup> or superconducting<sup>14</sup> behavior, other studies have concluded that

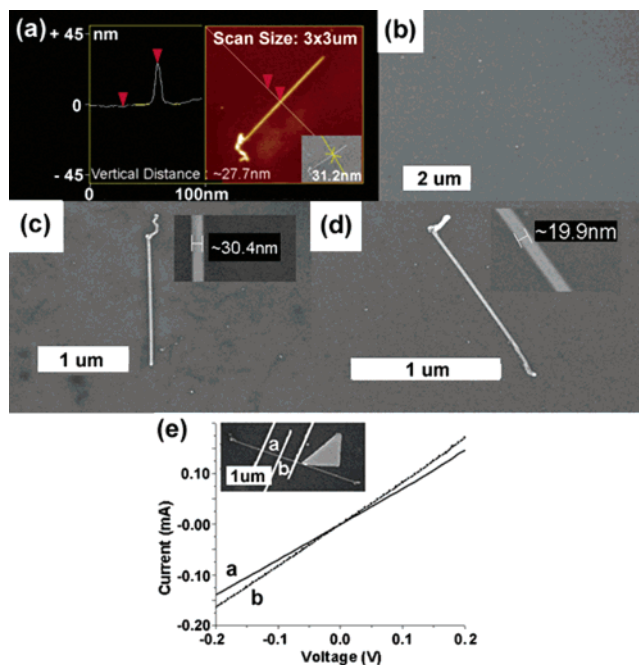


**Figure 5.** (a) Section profile AFM image of a silver nanowire templated on a 1D-3HB filament. (Inset) SEM image of the same nanowire. (b) Control experiment. Without DNA, we do not see any wire-like objects after the metallization process. (c) and (d) SEM images of  $\sim 30 \text{ nm}$  and  $\sim 20 \text{ nm}$  width silver nanowires. (e) Current–voltage measurement through a section of 1D-3HB templated silver nanowire. (Inset) an actual electronic device patterned by electron beam lithography.

DNA molecules are insulators.<sup>15,16</sup> Rather than relying on electrical transport through DNA itself, we have made use of DNA nanostructures as templates for the specific deposition of highly conductive metallic nanowires. Here we present 1D-3HB filament templated silver nanowires created using an electroless chemical deposition method (for details, see Supporting Information). We have previously reported on two distinct self-assembled nanostructures:  $4 \times 4$  tile nanoribbons<sup>3</sup> and TX nanotubes.<sup>6</sup> Both of these form tube-like superstructures, with diameters of  $\sim 40 \text{ nm}$  for nanoribbons and  $\sim 25 \text{ nm}$  for nanotubes. In contrast, 1D-3HB tiles form filaments which are a single tile wide with a diameter of  $\sim 4 \text{ nm}$ , therefore we expected to assemble thinner metallic nanowires after metallization than shown previously. Figure 5a shows an AFM image of the silver nanowire with section profile and SEM image of the same nanowire (inset) on a silicon substrate. The metallized nanowires showed widths of between 20 and 50 nm. The majority of nanowires have widths from 25 to 35 nm ( $\sim 70\%$ ), about 10% are narrower than 25 nm, and about 20% are wider than 35 nm, as measured by SEM. The average width of the silver nanowires is  $\sim 30 \text{ nm}$  and length is  $\sim 2 \mu\text{m}$ . Using widths measured by SEM and heights measured by AFM, the metallized nanowires appear slightly wider than their height. The average ratio of height to width is  $\sim 0.89$ . An SEM image of an example wire with width  $\sim 30 \text{ nm}$  is shown in Figure 5c and another with  $\sim 20 \text{ nm}$  width is shown in Figure 5d.

We performed conductivity measurements using metallized 1D-3HB nanowires at room temperature. Chromium–gold

double layer electrodes were deposited onto the nanowires by electron-beam lithography, with 5 nm of Cr followed by 25 nm of Au patterned onto the silicon substrate. An SEM image of a nanowire with attached electrodes is shown in Figure 5e (inset). The current–voltage ( $I$ – $V$ ) measurement was conducted on this device with electrode gap distances (wire lengths) of 430 nm, labeled as ‘a’, and 320 nm, ‘b’. The  $I$ – $V$  curves show mostly linear behavior (obey Ohm’s law) and give resistances of 1.42 k $\Omega$  for ‘a’ and 1.21 k $\Omega$  for ‘b’ measured at 0.1 V. These numbers correspond to bulk resistivities of  $2.25 \times 10^{-6} \Omega\text{-m}$  and  $2.57 \times 10^{-6} \Omega\text{-m}$  for ‘a’ and ‘b’ respectively. The bulk resistivity of polycrystalline silver is much lower ( $1.6 \times 10^{-8} \Omega\text{-m}$ ) than that of 1D-3HB templated nanowires. The nanowires’ higher resistivities may result from granularity of the silver structure and/or low-density silver packing around the 1D filaments. These nanowires demonstrate much higher conductivity than previously reported double-strand DNA templated silver nanowires,<sup>17</sup> although their conductivity is slightly lower than that reported for  $4 \times 4$  nanoribbon templated silver nanowires.<sup>3</sup> 3HB templated nanowires have a uniform average width of  $\sim 30$  nm with negligible granularity compared with the original report of dsDNA-templated silver nanowires by Braun et al., which gave  $\sim 100$  nm widths with clearly visible 30–50 nm grains.<sup>17</sup> The 3HB wires show  $\sim 25,000$  times lower resistance ( $\sim 1.2$  k $\Omega$ ) than Braun et al. ( $\sim 30$  M $\Omega$ ). Repeatable and reliable metallization processes and successful conductivity measurements show that we have taken a major step toward producing electronic nanodevices using DNA’s scaffolding capability and programmability.

In conclusion, we have designed and constructed novel DNA nanostructures, 1D- and 2D-three-helix bundle tiles that self-assemble into filaments and lattices. Uniform-width filaments served as templates for highly conductive metallic nanowires. Theoretically, they can also be used as templates for other materials such as semiconducting, superconducting, or magnetic nanowires, for a variety of applications in future electronic devices. We have also presented 2D lattices using slightly modified 3HB tiles. Unit tiles of 2D-3HB have an odd number of helical half-turns (4.5 full helical turns) and therefore present alternating stripes with the extra helix either above or below the lattice plane. With tile sets containing greater numbers of sticky-ends, 2D-3HB lattices could serve as addressable templates for protein or metallic nanoparticle period arrays for use in molecular machines or quantum dot

cellular automata. It might also be possible to attach protein-magnetic nanoparticle conjugates to these lattices for use as spintronic nanodevices.<sup>18,19</sup>

**Acknowledgment.** This work has been supported by grants CCF-0453686, CCF-0453685, CCR-0326157, EIA-0086015, and EIA-0218376 from the National Science Foundation. We thank Prof. Jie Liu for providing access to a Nanoscope IIIa AFM.

**Supporting Information Available:** DNA base sequences, experimental methods (including two step metallization procedure), additional AFM images, and image analysis. This material is available free of charge via the Internet at <http://pubs.acs.org>.

## References

- (1) Seeman, N. C. *Nature* **2003**, *421*, 427.
- (2) Turberfield, A. *Phys. World* **2003**, *16*, 43.
- (3) Yan, H.; Park, S. H.; Finkelstein, G.; Reif, J. H.; LaBean, T. H. *Science* **2003**, *301*, 1882.
- (4) Winfree, E.; Liu, F.; Wenzler, L. A.; Seeman, N. C. *Nature* **1998**, *394*, 539.
- (5) LaBean, T. H.; Yan, H.; Kopatsch, J.; Liu, F.; Winfree, E.; Reif, J. H.; Seeman, N. C. *J. Am. Chem. Soc.* **2000**, *122*, 1848.
- (6) Liu, D.; Park, S. H.; Reif, J. H.; LaBean, T. H. *Proc. Natl. Acad. Sci. U.S.A.* **2004**, *101*, 717.
- (7) Mao, C.; Sun, W.; Seeman, N. C. *J. Am. Chem. Soc.* **1999**, *121*, 5437.
- (8) Mao, C.; Sun, W.; Shen, Z.; Seeman, N. C. *Nature* **1999**, *397*, 144.
- (9) Yurke, B.; Turberfield, A. J.; Mills, A. P.; Simmel, F.; Neumann, J. L. *Nature* **2000**, *406*, 605.
- (10) Feng, L.; Park, S. H.; Reif, J. H.; Yan, H. *Angew. Chem., Int. Ed.* **2003**, *42*, 4342.
- (11) Mao, C.; LaBean, T. H.; Reif, J. H.; Seeman, N. C. *Nature* **2000**, *407*, 493.
- (12) Yan, H.; Feng, L.; LaBean, T. H.; Reif, J. H. *J. Am. Chem. Soc.* **2003**, *125*, 14246.
- (13) Porath, D.; Bezryadin, A.; de Vries, S.; Dekker, C. *Nature* **2000**, *403*, 635.
- (14) Kasumov, A.; Kociak, M.; Gueron, S.; Reulet, B.; Volkov, V. T.; Klinov, D. V.; Bouchiat, H. *Science* **2001**, *291*, 280.
- (15) Storm, A.; van Noort, J.; de Vries, S.; Dekker, C. *Appl. Phys. Lett.* **2001**, *79*, 3881.
- (16) de Pablo, P. J.; Moreno-Herrero, F.; Colchero, J.; Herrero, J.; Herrero, P.; Baro, A. M.; Ordejon, P.; Soler, J.; Artacho, E. *Phys. Rev. Lett.* **2000**, *85*, 4992.
- (17) Braun, E.; Eichen, Y.; Sivan, U.; Ben-Yoseph, G. *Nature* **1998**, *391*, 775.
- (18) Wolf, S. A.; Awschalom, D. D.; Buhrman, R. A.; Daughton, J. M.; von Molnar, S.; Roukes, M. L.; Chtchelkanova, A. Y.; Treger, D. M. *Science* **2001**, *294*, 1488.
- (19) Zwolak, M.; Di Ventra, M. *Appl. Phys. Lett.* **2002**, *81*, 925.

NL050108I